Study of $B^0 \to K^{*0}\tau\tau$ at FCC-ee

Tristan Miralles - FCC Clermont group

ECFA Flavour Physics meeting : 18th of April

1. Context

2. $B^0 \to K^*\tau^+\tau^-$ reconstruction method and vertexing emulation

3. Backgrounds, selection and precision determination

4. Detectors emulation

5. Results & outlook

$b \to s\tau\tau$ and objectives

- Third generation couplings in quark transitions are the less-well known.

- Specific models addressing the Flavour problem(s) often provide $b \to \tau$ enhancements or modifications w.r.t. the SM $\Rightarrow b \to s\tau\tau$ ($m_\tau \sim 20m_\mu$) is a must do to sort out the BSM models [1, 2]. Problem : measuring the ν's.

- SM : the $b \to s\tau\tau$ transition proceeds through an electroweak penguin diagram.

- Study of the rare heavy-flavoured decay $B^0 \to K^*\tau^+\tau^-$. SM prediction : BR=$\mathcal{O}(10^{-7}) \to$ not observed yet (present limit : $\mathcal{O}(10^{-3} - 10^{-4})$ [3]).
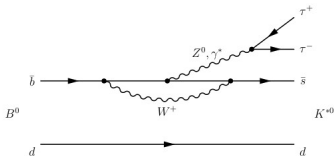
EW penguin quark-level transition

Topology

- The $B^0 \to K^*\tau\tau$ decay topology is driven by the tau decay multiplicity.
- There are from 2 to 4 neutrinos (not detected) and at least 4 charged particles in the final state and one, two, or three decay vertices.
- We focus on the 3-prongs tau decays ($\tau \to \pi\pi\pi\nu$) for which the decay vertex can be reconstructed in order to solve fully the kinematics.
- 10 particles in the final state ($K, 7\pi, \nu, \bar{\nu}$), 3 decay vertices and 2 undetected neutrinos.
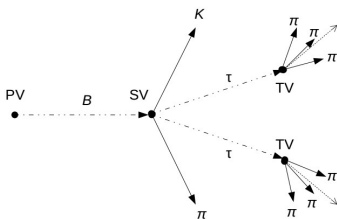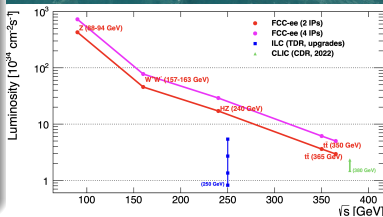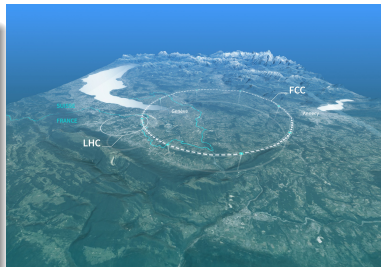

Decay topology

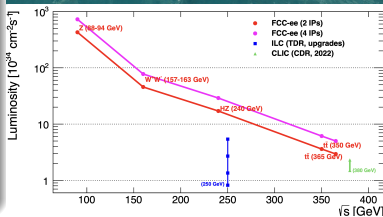Difficult to achieve SM value with current facilities → what about future facilities ?

FCC-*ee*

- FCC is a collider project at CERN of 91 km of circumference.

- FCC-*ee* is the first phase of the project with e^+e^- collisions.

- Four experiments in the FCC-*ee* baseline.

- Precision measurements at the four electroweak thresholds.

- Four data taking years expected at the Z pole $\Rightarrow 740 \times 10^9$ of $B^0/\bar{B}^0$.

- Combines a clear experimental environment (like B-factories) and boosted b-hadrons (like LHC).

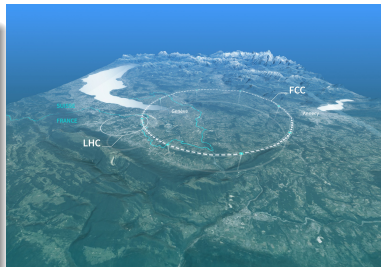- Looks like a good place to reconstruct the ν's.

FCC-*ee*

- FCC is a collider project at CERN of 91 km of circumference.
- FCC-*ee* is the first phase of the project with e^+e^- collisions.
- Four experiments in the FCC-*ee* baseline.
- Precision measurements at the four electroweak thresholds.
- Four data taking years expected at the Z pole $\Rightarrow 740 \times 10^9$ of $B^0/\bar{B}^0$.
- Combines a clear experimental environment (like B-factories) and boosted b-hadrons (like LHC).
- Looks like a good place to reconstruct the ν's.

Goal : explore the feasibility of the search for $B^0 \to K^* \tau^+ \tau^-$ at FCC-*ee* [4] and give the corresponding detector requirements.

Data and software used

- The events used in this work are generated with Pythia [5] ($Z \to b\bar{b}$ and hadronisation) and EvtGen [6] (forcing the decay with adequate models).

- The reconstruction is performed with the FCC Analyses sw using Delphes [7] simulation (featuring the IDEA [8] detector).

- The simulated data use tracks reconstructed with actual IDEA momentum resolution.

- Regarding the decay topology, the vertex resolution drives the feasibility of the measurement.

- Several vertexing performance working points will be tested and compared with the state-of-the-art (IDEA) one.
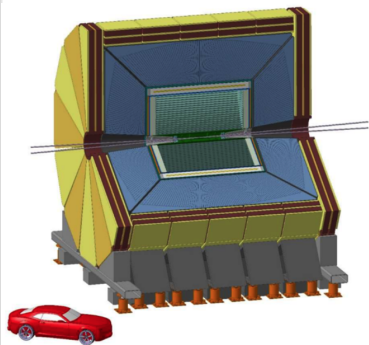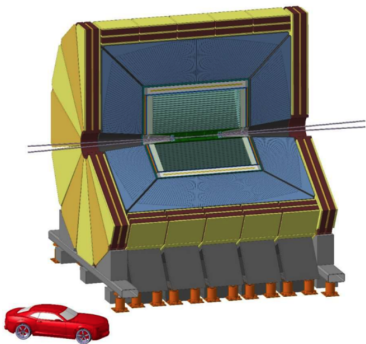

IDEA scheme.

Data and software used

- The events used in this work are generated with Pythia [5] ($Z \to b\bar{b}$ and hadronisation) and EvtGen [6] (forcing the decay with adequate models).

- The reconstruction is performed with the FCC Analyses sw using Delphes [7] simulation (featuring the IDEA [8] detector).

- The simulated data use tracks reconstructed with actual IDEA momentum resolution.

- Regarding the decay topology, the vertex resolution drives the feasibility of the measurement.

- Several vertexing performance working points will be tested and compared with the state-of-the-art (IDEA) one.

IDEA scheme.

Observable : BF measurement ; precision as a function of the vertex resolution.

Neutrinos reconstruction method

To fully reconstruct the kinematics of the decay (B invariant-mass observable for instance) we need :

- Momentum of all final particles, including not detected neutrinos.
- The decay lengths (6 constraints) together with the tau mass (2 constraints) can be used to determine the missing coordinates (6 degrees of freedom).
- We use energy-momentum conservation at tertiary (or τ decay) vertex with respect to τ direction [i].
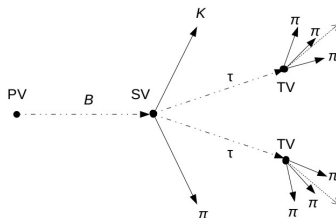
The dotted lines represent the non-reconstructed particles. The plain lines are the particles that can be reconstructed in the detector.

$$
\begin{cases}
p_{\nu_\tau}^\perp = -p_{\pi_t}^\perp \\
p_{\nu_\tau}^\parallel = \dfrac{((m_\tau^2 - m_{\pi_t}^2) - 2p_{\pi_t}^{\perp,2})}{2(p_{\pi_t}^{\perp,2} + m_{\pi_t}^2)} . p_{\pi_t}^\parallel \pm \dfrac{\sqrt{(m_\tau^2 - m_{\pi_t}^2)^2 - 4m_\tau^2 p_{\pi_t}^{\perp,2}}}{2(p_{\pi_t}^{\perp,2} + m_{\pi_t}^2)} . E_{\pi_t}
\end{cases}
$$

i. **Another way to do this computation is given by [9].**

Selection rule

- **There is a quadratic ambiguity on each neutrino momentum.**
- The ambiguities propagate to τ and B reconstructions.
- Four possibilities by taking all $+/-$ combinations for the two neutrinos.
- **A selection rule is needed to choose the right possibility.**
- From the energy-momentum conservation at the B decay vertex, we have a condition between the τ's and the K^* w.r.t. the B direction.

$$p_{\tau_-^+} = -\frac{\vec{p}_{K*}^{\perp}.\vec{e}_{\tau_-^+}}{1 - (\vec{e}_{\tau_-^+}.\vec{e}_B)^2} - p_{\tau_+^-}.\frac{\vec{e}_{\tau_+^+}.\vec{e}_{\tau_+^-} - (\vec{e}_{\tau_+^+}.\vec{e}_B)(\vec{e}_{\tau_-^-}.\vec{e}_B)}{1 - (\vec{e}_{\tau_-^+}.\vec{e}_B)^2}$$

Neutrinos reconstruction and selection rule validated at MC truth level.

Vertexing performance working points

- At the beginning of this study : no vertexing available → vertex resolutions emulated from MC truth.

- PV : 3D normal law including Beam Spot Constraints.

- SV & TV → ellipsoidal (decaying particle direction as reference) :
    - longitudinal,
    - transverse.

- Several working points examined (Longitudinal-Transverse configuration denoted as L-T in the following) :
    - 5 μm to 20 μm longitudinal,
    - 1 μm to 8 μm transverse.

- 20-3 (L-T) smearing used as reference in the following.

- Experimental vertexing efficiency is conservatively taken as 80% for the time being.
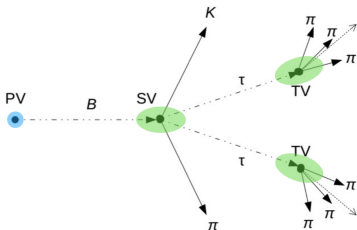
The considered backgrounds

- The relevant backgrounds are those with a final state similar to that of the signal ($K7\pi$).

- Several possible modes in $b \to c\bar{c}s$ and $b \to c\tau\nu$ transitions[ii], but often not observed to date $\Rightarrow$ guesstimates of the branching fractions from phase space computation and use of analogies.

- Determination of the dominant backgrounds for the measurement by estimating per-track efficiencies from 6 already generated backgrounds.

ii. **More details on backgrounds choices in appendix.**

The considered backgrounds

- The relevant backgrounds are those with a final state similar to that of the signal ($K7\pi$).

- Several possible modes in $b \to c\bar{c}s$ and $b \to c\tau\nu$ transitions[ii], but often not observed to date $\Rightarrow$ guesstimates of the branching fractions from phase space computation and use of analogies.

- Determination of the dominant backgrounds for the measurement by estimating per-track efficiencies from 6 already generated backgrounds.

Decay	BF (SM/meas.)	Intermediate decay	BF_had	Additional missing particles
Signal : $B^0 \to K^*\tau\tau$	1.30×10^{-7}	$\tau \to \pi\pi\pi\nu$, $K^* \to K\pi$	9.57×10^{-11}	
Backgrounds $b \to c\bar{c}s$:				
$B^0 \to K^{*0}D_sD_s$	5.47×10^{-5}	$D_s \to \tau\nu$	1.14×10^{-10}	2ν
		$D_s \to \tau\nu, \pi\pi\pi\pi^0$	1.28×10^{-10}	ν , π^0
		$D_s \to \pi\pi\pi\pi^0$	1.45×10^{-10}	$2\pi^0$
		$D_s \to \tau\nu, \pi\pi\pi\pi^0\pi^0$	1.08×10^{-9}	ν , $2\pi^0$
		$D_s \to \pi\pi\pi 2\pi^0$	1.02×10^{-8}	$4\pi^0$
$B^0 \to K^{*0}D_sD_s^*$	1.73×10^{-4}	$D_s \to \tau\nu$	3.60×10^{-8}	2ν, γ/π^0
		$D_s \to \pi\pi\pi\pi^0\pi^0$	3.22×10^{-8}	$4\pi^0$, γ/π^0
Backgrounds $b \to c\tau\nu$:				
$B^0 \to K^{*0}D_s\tau\nu$	9.17×10^{-6}	$D_s \to \tau\nu$	3.59×10^{-10}	2ν
$B^0 \to K^{*0}D_s^*\tau\nu$	2.03×10^{-5}	$D_s \to \pi\pi\pi\pi^0\pi^0$	7.51×10^{-9}	ν, γ, $2\pi^0$

ii. **More details on backgrounds choices in appendix.**

Landscape without selection

- The B^0 mass has been reconstructed for all modes.

- Calorimeter PID performances : π^0 detection rate of 80% is assumed in order to reduce the π^0 backgrounds.

- Backgrounds are overwhelming.

- An additional selection is required !

- We performed a multivariate selection : XGBoost [10].
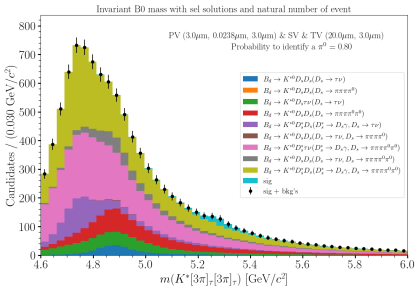
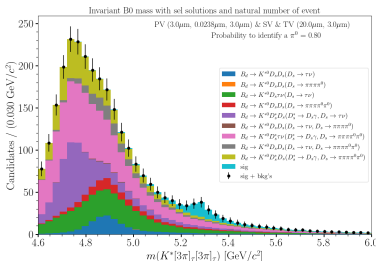| S/(S+B) [iii]	0.102

[iii]. **S/(S+B) is the purity evaluated on the [5.2, 5.6]GeV/c² window.**

Preselection

Variable	Cut
$m^2_{2\pi_{min}}$ & $m^2_{2\pi_{max}}$	< 0.3 & < 0.5 GeV
p_{K^*}	< 1GeV
$p_{3\pi}$	< 1GeV
$p_{\pi_{max}}$	< 0.25GeV
$p_{\pi_{min}}$	< 0.2GeV
FD_B	< 0.3mm
FD_τ	> 4mm
$m_{3\pi}$	< 0.750GeV
$m_{2\pi_{max}}$	< 0.5GeV
$m_{2\pi_{min}}$	> 1GeV

- Several kinematics variables have been saved for each events (like momentum or intermediate mass).

- Among them, discriminative variables have been found.

- The preselection has been built with these variables.

- The plot displays the result after preselection → the picture show a first improvement.

- The MVA can be trained against the backgrounds on the [5,5.6] GeV mass window.


S/(S+B)	0.307

MVA

- Training dataset generated with signal and the collection of available backgrounds.

- Backgrounds are considered in natural proportion (after the preselection).

- 50/50 split train/validation.

- The previous variables are given as input, as well as the reconstructed p_τ of each τ candidate.

- XGB parameters optimised on AUC.

- Overtraining plot to check the validity of the training $\rightarrow$ OK.

- Use of the MVA [iv] to perform the selection (cut at 0.5 on the BDT output) $\Rightarrow$ clearly better picture.

Invariant B0 mass with sel solutions and natural number of event
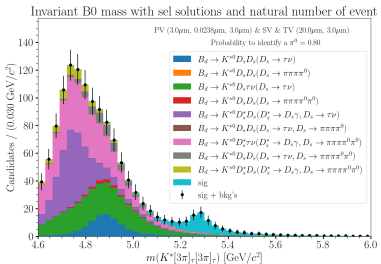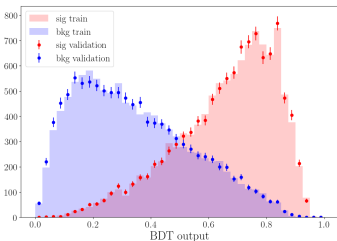
S/(S+B)	0.753


iv. Feature importance plot in appendix.

Determination of the measurement precision

- Same selection applied to all vertex resolution emulations.

- Unbinned ML fit of the data with :
  - signal → double CB + a Gaussian,
  - background → two decreasing exponential.

- Fitting scheme :
  1. fit of the simulated signal
  2. fit of the signal and background rescaled w.r.t. their yields

- Extraction of the signal yield N and the associated error σ_N.

- Precision of the BF measurement of $B^0 \to K^{*0}\tau\tau$ given by σ_N/N.

A RooPlot of "mass"
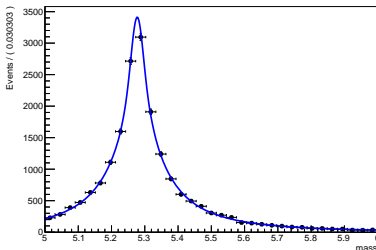
A RooPlot of "mass"
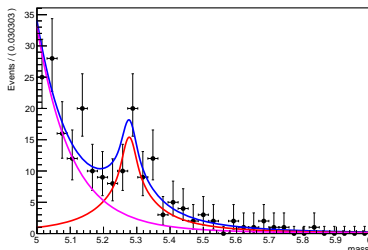
Precision of the measurement
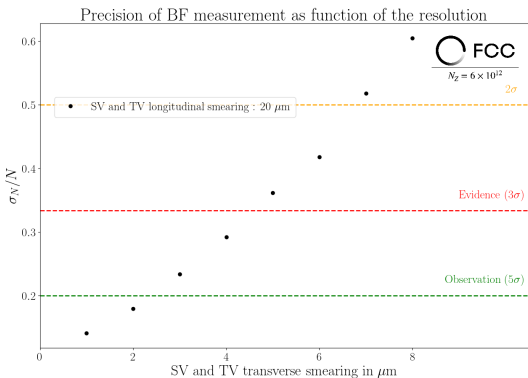
Precision of BF measurement as function of the resolution

Emulation of the vertex resolution performances in order to look for the feasibility of the search of $B^0 \to K^{*0}\tau\tau$ at FCC-ee :

- possible with the best arbitrary working points,
- **where is the state of the art ?**

The IDEA working point : primary vertex resolution

- Resolutions determined from 10^6 signal events.

- Reconstructed PV position fitted from reconstructed tracks with the FCCAnalyses VertexFitterSimple tools (Beam Spot Constraints set at $(4.5, 20e^{-3}, 300)\mu m$).

- Displacement of the reconstructed PV w.r.t. the MC truth PV is built in Cartesian coordinates.

- The IDEA PV resolution is determined for each coordinate by a fit of the displacement : use of double (x,z[v]) or simple (y) Gaussian model.

- Resolutions $\mathcal{O}(3\,\mu m)$ for (x,z).

- Resolution $\mathcal{O}(20\,nm)$ for y.

v. In appendix.
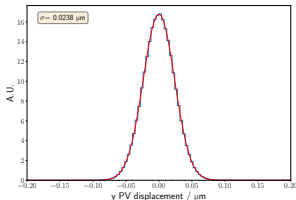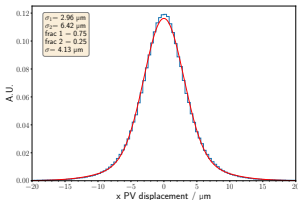
PV displacement and fit of the resolution for x (top) and y (bottom).

The IDEA working point : secondary and tertiary vertices resolutions

- Reconstructed SV ($K^{*0} \to K\pi$) and TV ($\tau \to 3\pi$) positions fitted from MC matched reconstructed tracks via FCCAnalyses VertexFitterSimple tools.

- Displacement of the reconstructed SV and TV w.r.t. to the MC truth projected on decay plan (L-T).

- Signed decomposition of the transverse displacement determined from two orthogonal directions pick-up randomly via a circle parameterized in the transverse plan itself.

- The IDEA resolution is determined for each coordinate by a fit of the displacement with a triple-Gaussian model.
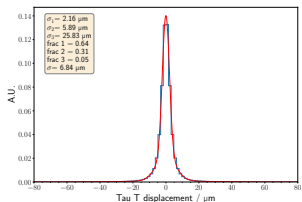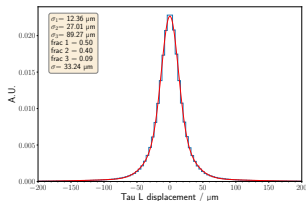
TV displacement and fit of the resolution for L (top) and T (bottom) directions.

The IDEA working point : emulation

- Emulation of the PV resolutions with 3D-gaussian smearing that follow the combined σ of the fits among each axis.
- SV and TV smearing via the IDEA fitted resolutions.
- Smearing emulated on each direction via accept/reject algorithms.

Additional working points

- The SmearObjects.SmearedTracks tools allows to use IDEA vertexing with direct tracks improvements.
- 4 various IDEA working points examined with better Ω (momentum) or IP resolutions.
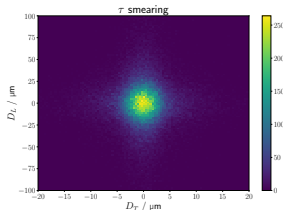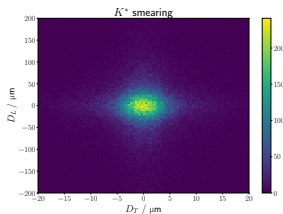
Example of 2D smearing used to emulate the SV (top) and TV (bottom) IDEA resolutions.

IDEA precision
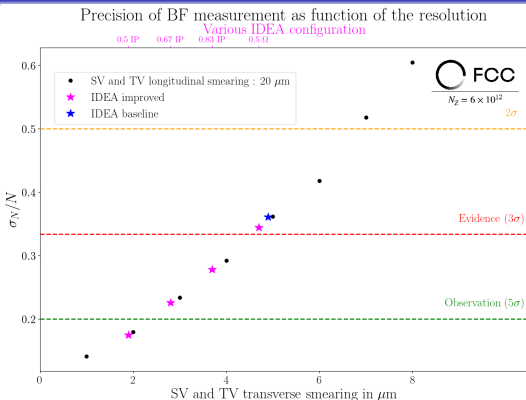
Precision of BF measurement as function of the resolution

Emulation of the vertex resolution performances in order to look for the feasibility of the search of $B^0 \to K^{*0}\tau\tau$ at FCC-*ee* :

- IDEA baseline close to the evidence,
- IP measurements improvement could helps a lot $\Rightarrow$ but what does it means in term of detector ?

How to practically improve IP resolutions

- Samples with improved detector in term of single hit resolution (from $3\,\mu m$ to $2\,\mu m$ for the barrel layers) or material budget in the vertex detector layers and beam pipe (-50%) have been simulated.

- **Goal** : check if regular detectors improvements are consistent with the expectations from d_0 resolution fits [vi] with :

$$\sigma_{d_0} = \frac{a(\sqrt{x/X_0})}{p_T} + b(\text{geometry}).$$

- The single hit resolution improvement is, as expected, linearly correlated to the offset of the resolution.

- The material budget reduction is close to the expected $\sqrt{x/X_0}$ slope improvement if the vertex detector and the beam pipe are both concerned.

- Next step : emulation of these new points.

---

vi. **Detailed equation in appendix.**

Results

Precision of BF measurement as function of the resolution
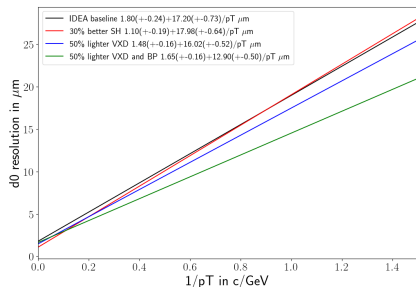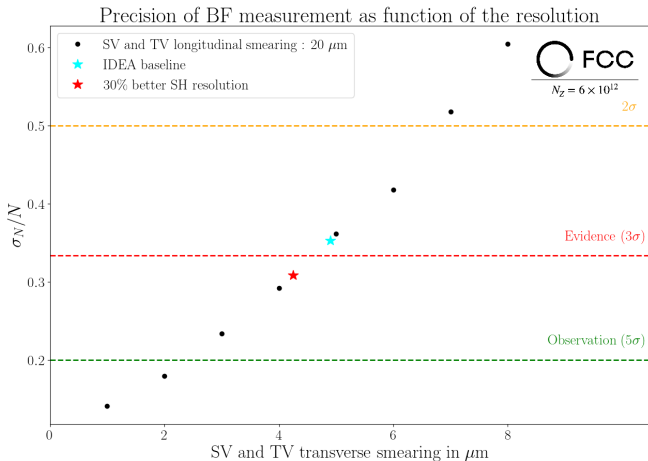
The 30 % single hit resolution improvement allow to reach the 3σ threshold.

Results

Precision of BF measurement as function of the resolution
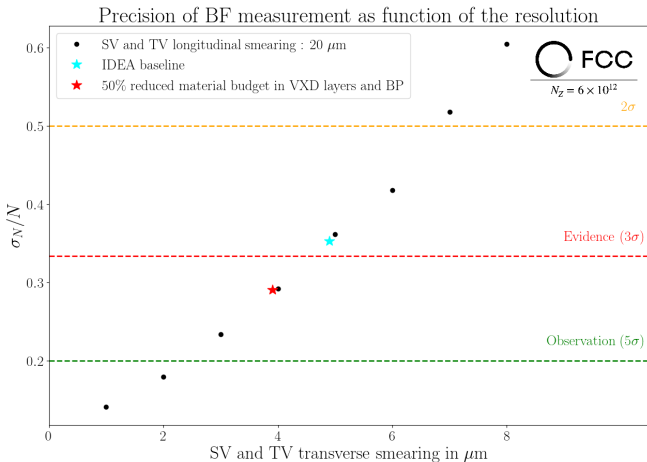
Vertex resolution is dominated by multiple Coulombian scatterings and already limited by the beam pipe material.

Conclusion

Last words

- Analysis aimed at assessing the required vertexing performances to measure $B^0 \to K^{*0}\tau\tau$ from the two $\tau \to 3\pi$ self-contained method only.

- Very demanding...

- The main reconstruction limitation, w.r.t. vertex detector, comes from material budget in the beam pipe.

Conclusion

Last words

- Analysis aimed at assessing the required vertexing performances to measure $B^0 \to K^{*0}\tau\tau$ from the two $\tau \to 3\pi$ self-contained method only.

- Very demanding...

- The main reconstruction limitation, w.r.t. vertex detector, comes from material budget in the beam pipe.

Outlook

- Considering τ leptonic decays on one (both) branch(es) brings a factor 7 (14) in statistics but require(s) other reconstruction method(s).

Context | Reconstruction and vertexing emulation | Backgrounds, selection and precision | Detectors emulation | **Results & outlook**

oooo | oooooooo | oooooo | ooooo | ooo●

Conclusion

Last words

- Analysis aimed at assessing the required vertexing performances to measure $B^0 \to K^{*0}\tau\tau$ from the two $\tau \to 3\pi$ self-contained method only.
- Very demanding...
- The main reconstruction limitation, w.r.t. vertex detector, comes from material budget in the beam pipe.

Outlook

- Considering τ leptonic decays on one (both) branch(es) brings a factor 7 (14) in statistics but require(s) other reconstruction method(s).

Thanks !

Expected number of events

The knowledge of the reconstruction efficiency allows us to compute the expected number of B^0 decays fully reconstructed at FCC-ee :

$$\mathcal{N}_{K^*\tau\tau \to K7\pi2\nu} = \mathcal{N}_Z.BR(Z \to b\bar{b}).2f_d.BR(K^*\tau\tau).BR(\tau \to \pi\pi\pi\nu)^2.BR(K^* \to K\pi).\epsilon_{reco}.\epsilon_{vertex}$$

Where :

- $\mathcal{N}_Z = 6 \times 10^{12}$ the expected number of Z produced,
- $BR(Z \to b\bar{b}) = 0.1512 \pm 0.0005$,
- $f_d = 0.407 \pm 0.007$ the hadronisation term,
- $BR(K^*\tau\tau) = 1.30 \times 10^{-7} \pm 10\%$ the SM predicted branching fraction,
- $BR(\tau \to \pi\pi\pi\nu) = 0.0931 \pm 0.0005$,
- $BR(K^* \to K\pi) = 0.69$,
- $\epsilon_{reco} = 0.3840 \pm 0.0007$ for a smearing $3\,\mu m - 20\,\mu m$,
- $\epsilon_{vertex} = 0.8$,

$$\Rightarrow \mathcal{N}_{K^*\tau\tau \to K7\pi2\nu} \approx 176 \pm 18$$

Some words about guesstimation of the BF for unseen modes

- $B^0 \to K^{*0} D_s D_s$ from analogy game and form factors / phase space corrections :

$$BF(B^0 \to K^{*0} D_s D_s) = BF(B^+ \to K^+ D_s^+ D_s^-) \times C_{\mathrm{FF}} \times C_{\mathrm{PS}}$$

where $B^+ \to K^+ D_s D_s$ (recently measured by LHCb) has the same quark content than $B^0 \to K^{*0} D_s D_s$ but the spectator quark.

- Form factor correction K vs K^* from :

$$C_{\mathrm{FF}} = \frac{\mathrm{FF}_{\mathrm{K}^*}}{\mathrm{FF}_{\mathrm{K}}} = \frac{BF(B^+ \to D^0 K^{*+})}{BF(B^+ \to D^0 K^+)}.$$

- Phase space K vs K^*, from PS computed numerically (three body decay hypothesis used conservatively) :

$$C_{\mathrm{PS}} = \frac{PS(B^+ \to K^{*+} D_s^+ D_s^-)}{PS(B^+ \to K^+ D_s^+ D_s^-)}.$$

- $B^0 \to K^{*0} D_s^* D_s$ and $B^0 \to K^{*0} D_s^* D_s^*$ w.r.t. $B^0 \to K^{*0} D_s D_s$ from $B_s^0 \to D_s^{(*)} D_s^{(*)}$ hierarchy.

Some words about guesstimation of the BF for unseen modes

- $B^0 \to K^{*0} D_s^{(*)} \tau \nu$ from analogy via phase space computation [9] :

$$BF(B^0 \to K^{*0} D_s^{(*)} \tau \nu) = BF(B^+ \to K D_s^{(*)} \ell \nu) \times \frac{PS(B^0 \to K^{*0} D_s^{(*)} \tau \nu)}{PS(B^+ \to K D_s^{(*)} \ell \nu)}$$

  where PS denotes the Phase Space computed numerricaly (three body decay hypothesis used conservatively) and $B^+ \to K D_s^{(*)} \ell \nu$ is a reference mode with a known BF.

- $B^0 \to K^{*0} D_s \tau \nu$ and $B^0 \to K^{*0} D_s^* \tau \nu$ w.r.t $B^0 \to K^{*0} D_s^{(*)} \tau \nu$ from $B^0 \to D^{(*)} \ell \nu$ hierarchy.

- $B_s^0 \to K^{*0} D^{(*)} \tau \nu$ from analogy via phase space computation [9] :

$$BF(B_s^0 \to K^{*0} D^{(*)} \tau \nu) = BF(B_s^0 \to D_{s1} \mu \nu) \times \frac{PS(B_s^0 \to K^{*0} D^{(*)} \tau \nu)}{PS(B_s^0 \to D_{s1} \mu \nu)}$$

  where PS denotes the Phase Space computed numerically (three body decay hypothesis used conservatively) and $B_s^0 \to D_{s1} \mu \nu$ is a reference mode with a known BF.

- $B_s^0 \to K^{*0} D \tau \nu$ and $B_s^0 \to K^{*0} D^* \tau \nu$ w.r.t. $B_s^0 \to K^{*0} D^{(*)} \tau \nu$ from $B^0 \to D^{(*)} \ell \nu$ hierarchy.

Extended background table

Decay	BF (SM/meas.)	Intermediate decay	BF_had	Additional missing particles
Signal : $B^0 \to K^* \tau\tau$	1.30×10^{-7}	$\tau \to \pi\pi\pi\nu$, $K^* \to K\pi$	9.57×10^{-11}	
Backgrounds $b \to c\bar{c}s$:				
$B^0 \to K^{*0} D_s D_s$	5.47×10^{-5}	$D_s \to \tau\nu$	1.14×10^{-10}	2ν
		$D_s \to \tau\nu, \pi\pi\pi\pi^0$ [vii]	1.28×10^{-10}	ν , π^0
		$D_s \to \pi\pi\pi\pi^0$ [vii]	1.45×10^{-10}	$2\pi^0$
		$D_s \to \tau\nu, \pi\pi\pi\pi^0\pi^0$	1.08×10^{-9}	ν , $2\pi^0$
		$D_s \to \pi\pi\pi 2\pi^0$ [vii]	1.02×10^{-8}	$4\pi^0$
$B^0 \to K^{*0} D_s D_s^*$	1.73×10^{-4}	$D_s \to \tau\nu$	3.60×10^{-10}	$2\nu, \gamma/\pi^0$
		$D_s \to \tau\nu, \pi\pi\pi\pi^0$	4.06×10^{-10}	ν , π^0, γ/π^0
		$D_s \to \pi\pi\pi\pi^0$	4.57×10^{-10}	$2\pi^0, \gamma/\pi^0$
		$D_s \to \pi\pi\pi\pi^0\pi^0$	3.22×10^{-8}	$4\pi^0, \gamma/\pi^0$
$B^0 \to K^{*0} D_s^* D_s^*$	1.79×10^{-4}	$D_s \to \tau\nu$	3.73×10^{-10}	$2\nu, 2\gamma/\pi^0$
		$D_s \to \tau\nu, \pi\pi\pi\pi^0$	4.20×10^{-10}	ν , π^0, $2\gamma/\pi^0$
		$D_s \to \pi\pi\pi\pi^0$	4.73×10^{-10}	$2\pi^0, 2\gamma/\pi^0$
Backgrounds $b \to c\tau\nu$:				
$B_s \to K^{*0} D\tau\nu$	7.27×10^{-5}	$D \to \pi\pi\pi\pi^0$	1.65×10^{-9}	ν, π^0
$B_s \to K^{*0} D^*\tau\nu$	2.03×10^{-4}	$D^* \to D^0\pi, D\pi^0$		
		$D \to \pi\pi\pi\pi^0$	1.12×10^{-9}	$\nu, 2\pi^0$
		$D^0 \to 2\pi 2\pi\pi^0$	8.98×10^{-10}	$\nu, 2\pi^0, 2\pi^\pm$
$\overline{B^0} \to \overline{K}^{*0}\overline{D_s}\tau\nu$	9.17×10^{-6}	$\overline{D_s} \to \tau\nu$	3.59×10^{-10}	2ν
		$D_s \to \pi\pi\pi\pi^0$	4.05×10^{-10}	ν, π^0
$B^0 \to K^{*0} D_s^*\tau\nu$	2.03×10^{-5}	$D_s \to \tau\nu$	8.07×10^{-10}	$2\nu, \gamma/\pi^0$
		$D_s \to \pi\pi\pi\pi^0$	9.09×10^{-10}	ν , π^0, γ/π^0
		$D_s \to \pi\pi\pi\pi^0\pi^0$	7.51×10^{-9}	$\nu, \gamma, 2\pi^0$

vii. $D_s \to 3\pi n\pi^0$ modes involve η/ω intermediate states.

Update of the $D_s \to \pi\pi\pi n\pi^0$ simulation

Better simulations for $D_s \to \pi\pi\pi n\pi^0$

- Previously this decay has been generated in the Phase Space $\to$ a more accurate simulation of the decay is needed $\Rightarrow$ new samples which include η/ω (saturating the inclusive BF) intermediate states are in order.

- Replacement of the previous samples.

- $B^0 \to K^{*0}D_sD_s(D_s \to \pi\pi\pi\pi^0)$ is now $B^0 \to K^{*0}D_sD_s$ where $D_s \to \eta/\omega\pi$ and $\eta/\omega \to \pi\pi\pi^0$.

- $B^0 \to K^{*0}D_sD_s(D_s \to \pi\pi\pi\pi^0\pi^0)$ is now $B^0 \to K^{*0}D_sD_s$ where $D_s \to \eta/\omega\pi\pi^0$ and $\eta/\omega \to \pi\pi\pi^0$.

Distribution of π^0 momentum from $D_s \to 3\pi 2\pi^0$

Momentum and transverse momentum distributions of the π^0
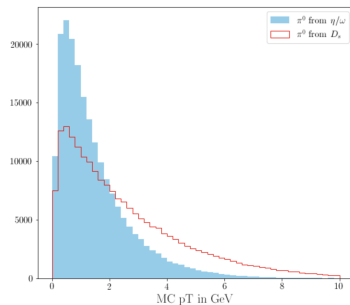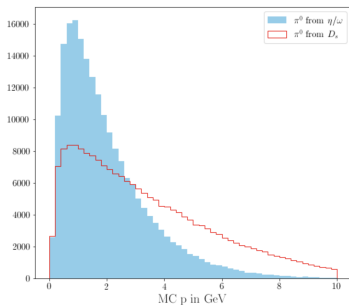
Distribution of π^0 momentum from $D_s \to 3\pi 2\pi^0$.

Some word about the choice of background to consider

- $B^0 \to K^{*0} D_s D_s$ with the two D_s decaying as $D_s \to \tau\nu$, $D_s \to \pi\pi\pi^0$ and $D_s \to \pi\pi\pi^0\pi^0$ already generated.
- $B^0 \to K^{*0} D_s^* D_s$ with the two D_s decaying as $D_s \to \tau\nu$ already generated.
- $B^0 \to K^{*0} D_s D_s$ with both $D_s \to \tau\nu$ and $D_s \to \pi\pi\pi^0$ already generated.
- Construction of a "per track" efficiency by taking the square root of the reconstruction efficiency of the four first modes $\Rightarrow \epsilon(D_s \to \tau\nu)$, $\epsilon(D_s^* \to \tau\nu)$, $\epsilon(D_s \to \pi\pi\pi^0)$ and $\epsilon(D_s \to \pi\pi\pi^0\pi^0)$.
- Cross-check : $\epsilon(D_s \to \tau\nu) \times \epsilon(D_s \to \pi\pi\pi^0) \simeq \epsilon(B^0 \to K^{*0} D_s D_s, D_s \to \tau\nu, D_s \to \pi\pi\pi^0)$.
- Construction of an $\epsilon(*) = \epsilon(D_s^* \to \tau\nu)/\epsilon(D_s \to \tau\nu)$.
- Computation of an estimated efficiency for the possible background from these per-track efficiencies.
- Ranking of the backgrounds via $BF \times \epsilon$.
- Choice of the biggest one for each type of specific topology.

Reconstruction efficiency

Mode	Total reconstruction efficiency (%)
Signal	38.40 ± 0.07
$B^0 \to K^{*0} D_s D_s, D_s \to \tau \nu$	47.49 ± 0.04
$B^0 \to K^{*0} D_s D_s, D_s \to 3\pi\pi^0$	2.190 ± 0.002
$B^0 \to K^{*0} D_s D_s, D_s \to 3\pi 2\pi^0$	56.30 ± 0.05
$B^0 \to K^{*0} D_s D_s, D_s \to \tau\nu/3\pi\pi^0$	10.14 ± 0.01
$B^0 \to K^{*0} D_s D_s, D_s \to \tau\nu/3\pi 2\pi^0$	51.64 ± 0.04
$B^0 \to K^{*0} D_s^* D_s, D_s \to \tau\nu$	48.27 ± 0.04
$B^0 \to K^{*0} D_s^* D_s, D_s \to 3\pi 2\pi^0$	57.30 ± 0.04
$B^0 \to K^{*0} D_s \tau\nu, D_s \to \tau\nu$	42.85 ± 0.04
$B^0 \to K^{*0} D_s^* \tau\nu, D_s \to 3\pi 2\pi^0$	47.26 ± 0.04

Summary table of the total reconstruction (including the B^0 candidate building and neutrino reconstruction) efficiency as function of the mode for the reference vertexing performances working point.
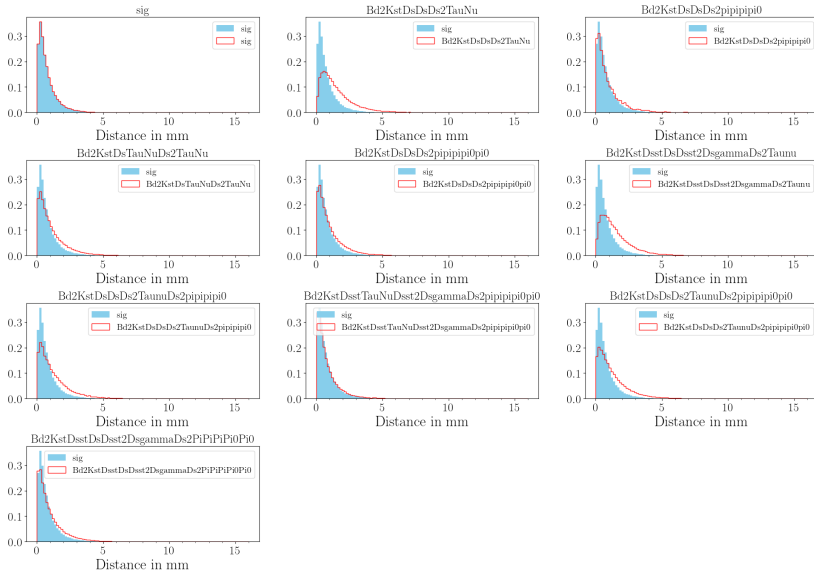
Reconstructed p_{tau} distribution signal vs backgrounds $20 - 3$ configuration
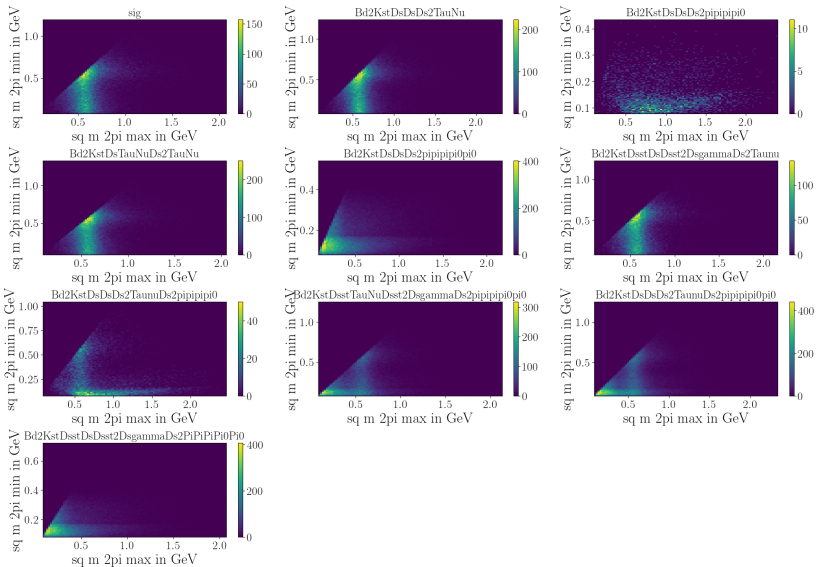

sel 20-3 P tau
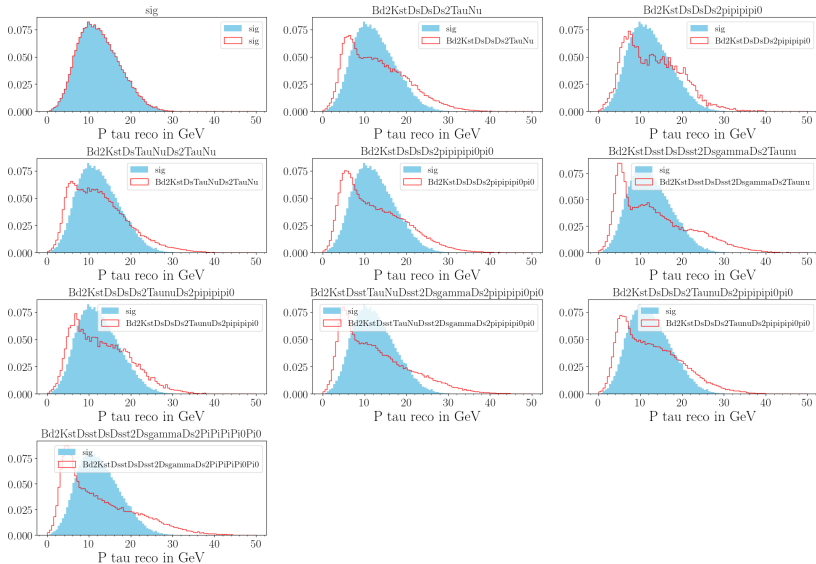
FD_τ distribution signal vs backgrounds $20-3$ configuration

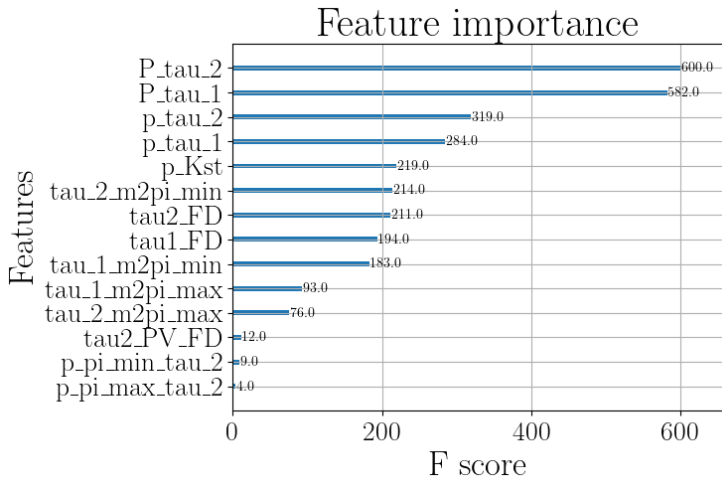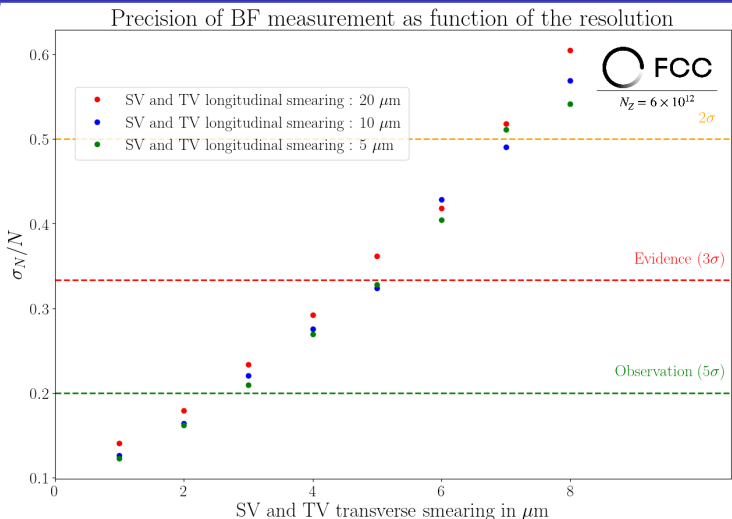sel 20-3 tau FD

Dalitz plane $(m^2_{\pi_{max}}, m^2_{\pi_{min}})$ signal and backgrounds $20 - 3$ configuration

XGB features importance's

Feature importance

Precision of the measurement with other longitudinal resolutions.

Precision of BF measurement as function of the resolution

Precision on the BF measurement as function of the vertex resolution with 3 longitudinal configurations. The observed hierarchy issue arises from the interplay between the smearing of the vertexing and the fit model.

Other IDEA resolution plots

σ_1= 1.72 µm
σ_2= 5.75 µm
frac 1 = 0.81
frac 2 = 0.19
σ= 2.93 µm
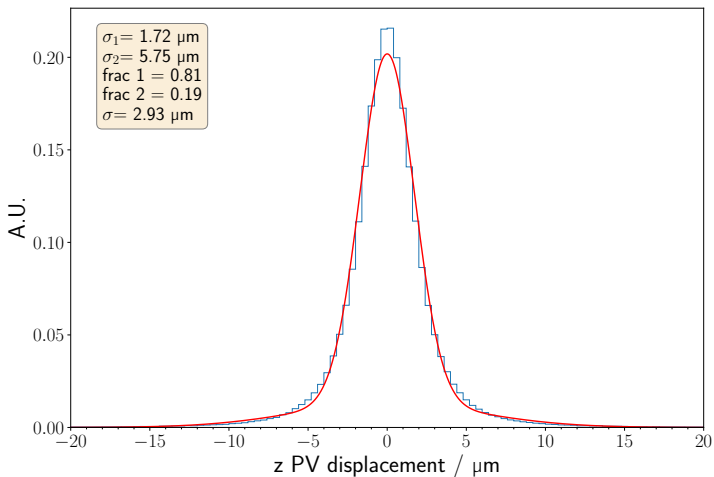
PV displacement and fit of the resolution for z

Other IDEA resolution plots
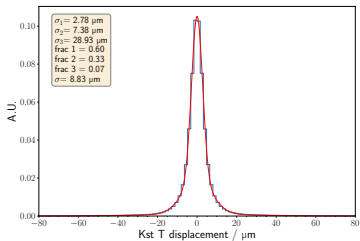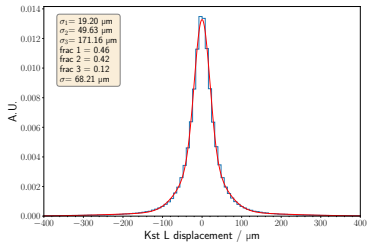
SV displacement and fit of the resolution for L (top) and T (bottom).

More detailed about IP resolution

Complete equation :

$$\sigma_{d_0} \simeq \sqrt{\frac{r_2^2 \sigma_1^2 + r_1^2 \sigma_2^2}{(r_2 - r_1)^2}} \oplus \frac{r}{p_T \sin^{1/2} \theta} 13.6 \, \text{MeV} \sqrt{\frac{x}{X_0}},$$

where the first term is link to detector resolution and the second to multiple scattering. $r_{1(2)}$ is the distance between the first (second) hit of the track and the PV, $\sigma_{1(2)}$ is the resolution on the first (second) hit of the track. r is the distance between the PV and the contact points of the track with the vertex detector layer, p_T is the transverse momentum of the track, θ is the polar angle of the track, x is the thickness, and X_0 is the radiation length.

📄 Paul Langacker.
The physics of heavy z' gauge bosons.
Reviews of Modern Physics, 81(3) :1199, 2009.

📄 I Dorsner, S Fajfer, A Greljo, JF Kamenik, and N Kosnik.
Physics of leptoquarks in precision experiments and at particle colliders.
Physics Reports, 641 :1–68, 2016.

📄 BABAR Collaboration et al.
Search for b+-> k+ tau (+) tau (-) at the babar experiment.
Physical Review Letters, 2017, vol. 118, num. 3, p. 031802, 2017.

📄 JF Kamenik, S Monteil, A Semkiv, and L Vale Silva.
Lepton polarization asymmetries in rare semi-tauonic $b \rightarrow s$ $b \rightarrow s$ exclusive decays at fcc-ee.
The European Physical Journal C, 77(10) :1–19, 2017.

📄 Torbjörn Sjöstrand, Stefan Ask, Jesper R Christiansen, Richard Corke, Nishita Desai, Philip Ilten, Stephen Mrenna, Stefan Prestel, Christine O Rasmussen, and Peter Z Skands.
An introduction to pythia 8.2.
Computer physics communications, 191 :159–177, 2015.

📄 Anders Ryd, David Lange, Natalia Kuznetsova, Sophie Versille, Marcello Rotondo, DP Kirkby, FK Wuerthwein, and A Ishikawa.
Evtgen : a monte carlo generator for b-physics.
BAD, 522 :v6, 2005.

📄 J De Favereau, Christophe Delaere, Pavel Demin, Andrea Giammanco, Vincent Lemaitre, Alexandre Mertens, Michele Selvaggi, Delphes 3 Collaboration, et al.
Delphes 3 : a modular framework for fast simulation of a generic collider experiment.
Journal of High Energy Physics, 2014(2) :57, 2014.

📄 CERN.
2nd fcc-france workshop, jan 20-21, 2021.
https:...Physics.pdf.

📄 Lingfeng Li and Tao Liu.
$b \to s\tau + \tau$- physics at future z factories.
Journal of High Energy Physics, 2021(6) :1–31, 2021.

📄 Tianqi Chen and Carlos Guestrin.
Xgboost : A scalable tree boosting system.
In *Proceedings of the 22nd acm sigkdd international conference on knowledge discovery and data mining*, pages 785–794, 2016.